

UNCOVERING EXTREMELY METAL-POOR STARS IN THE MILKY WAY'S ULTRA-FAINT DWARF SPHEROIDAL SATELLITE GALAXIES¹

EVAN N. KIRBY², JOSHUA D. SIMON³, MARLA GEHA⁴, PURAGRA GUHATHAKURTA², AND ANNA FREBEL⁵

Accepted for publication in ApJL

ABSTRACT

We present new metallicity measurements for 298 individual red giant branch stars in eight of the least luminous dwarf spheroidal galaxies (dSphs) in the Milky Way (MW) system. Our technique is based on medium resolution Keck/DEIMOS spectroscopy coupled with spectral synthesis. We present the first spectroscopic metallicities at $[\text{Fe}/\text{H}] < -3.0$ of stars in a dwarf galaxy, with individual stellar metallicities as low as $[\text{Fe}/\text{H}] = -3.3$. Because our $[\text{Fe}/\text{H}]$ measurements are not tied to empirical metallicity calibrators and are sensitive to arbitrarily low metallicities, we are able to probe this extremely metal-poor regime accurately. The metallicity distribution of stars in these dSphs is similar to the MW halo at the metal-poor end. We also demonstrate that the luminosity-metallicity relation previously seen in more luminous dSph galaxies ($M_V = -13.4$ to -8.8) extends smoothly down to an absolute magnitude of $M_V = -3.7$. The discovery of extremely metal-poor stars in dSphs lends support to the Λ CDM galaxy assembly paradigm wherein dwarf galaxies dissolve to form the stellar halo of the MW.

Subject headings: galaxies: dwarf — galaxies: abundances — Galaxy: halo — Galaxy: evolution — Local Group

1. INTRODUCTION

In the hierarchical theory of the assembly of galaxy halos (White & Rees 1978; Searle & Zinn 1978), dwarf galaxies interact gravitationally with their hosts, shedding stars, losing gas, and eventually tidally dissolving into the diffuse halo. Recent numerical simulations and semi-analytic models (e.g., Bullock & Johnston 2005) suggest that a Milky Way-like halo can be explained entirely by disrupted satellites in the Λ CDM paradigm.

Clearly, dwarf galaxies must play some role in building stellar halos of large galaxies because both the Milky Way (MW) and M31 exhibit tidal streams (e.g., Ibata et al. 2001; Choi et al. 2002; Gilbert et al. 2007) and dwarf galaxies in various stages of disruption (e.g., Ibata et al. 1994; Howley et al. 2008). However, the chemical abundances of individual stars in present-day MW dSphs do not match that of the MW halo. Shetrone et al. (2001) found a lower $[\alpha/\text{Fe}]$ for dSph red giant branch (RGB) stars than for MW halo RGB stars. The differences in chemical abundances led Tolstoy et al. (2003) to conclude that the bulk of the halo can not be composed of stars like those present in surviving dSphs.

In order to compare the bulk metallicities of stars in dSphs and the MW halo, Helmi et al. (2006, hereafter H06) obtained medium-resolution spectra of the MW dSphs Sculptor, Fornax, Sextans, and Carina. Using

an empirical relation between the infrared Ca II triplet (CaT) equivalent width (EW) and $[\text{Fe}/\text{H}]$ (Tolstoy et al. 2001), H06 find a lack of $[\text{Fe}/\text{H}] < -3.0$ stars in these four MW dSphs. Given this absence, they concluded that the MW halo, which contains numerous such stars, could not have formed from present-day dSphs. Nevertheless, dSphs could still be the building blocks if they once contained a population of extremely metal-poor stars. However, it remains difficult to understand how they could have lost *all* of those stars by now.

In this Letter, we revisit the absence of metal-poor stars in MW dSphs by targeting lower luminosity galaxies and by using a more direct technique to measure $[\text{Fe}/\text{H}]$ (based on Fe lines) than has been used before on low or moderate resolution spectra. In §2, we describe new metallicity measurements from the Simon & Geha (2007, hereafter SG07) data set of eight of the least luminous MW dSphs. As a result, we report for the first time the discovery of extremely metal-poor stars ($[\text{Fe}/\text{H}] < -3.0$) in MW dSphs. In §3, we compare the ultra-faint dSph MDF to the halo MDF. We also present the luminosity-metallicity relation for the full range of MW dSph luminosities. In §4, we briefly summarize our findings and discuss work on dSph chemical abundances beyond $[\text{Fe}/\text{H}]$.

2. METALLICITY MEASUREMENTS

We make use of the observations of SG07, who targeted eight of the ultra-faint dSphs discovered with SDSS: Coma Berenices, Canes Venatici I and II, Hercules, Leo IV, Leo T, and Ursa Major I and II. In summary, SG07 used DEIMOS on the Keck II telescope to obtain spectra at $R \sim 6000$ over a spectral range of roughly 6500–9000 Å. [See Guhathakurta et al. (2006) for details on the spectrograph configuration.] S/N varied widely from 5–120 Å^{−1}.

2.1. Technique

¹ Data herein were obtained at the W. M. Keck Observatory, which is operated as a scientific partnership among the California Institute of Technology, the University of California, and NASA. The Observatory was made possible by the generous financial support of the W. M. Keck Foundation.

² University of California Observatories/Lick Observatory, Department of Astronomy & Astrophysics, University of California, Santa Cruz, CA 95064; ekirby@ucolick.org

³ Department of Astronomy, California Institute of Technology, 1200 E. California Blvd., MS 105-24, Pasadena, CA 91125

⁴ Astronomy Department, Yale University, P.O. Box 208101, New Haven, CT 06520

⁵ McDonald Observatory, University of Texas, Austin, TX 78712

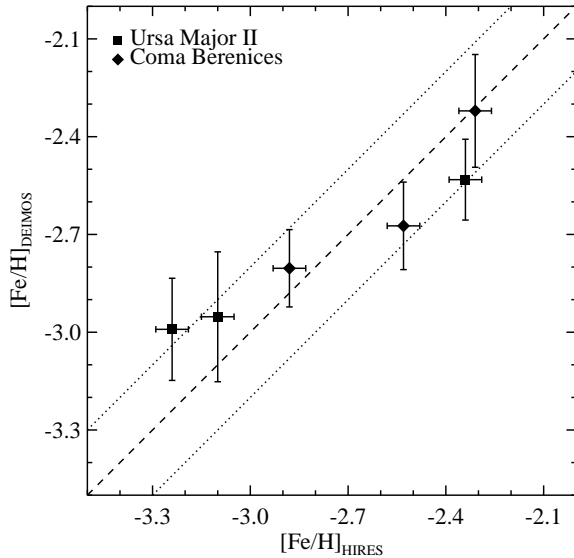


FIG. 1.— Metallicities for the RGB stars in two ultra-faint dSphs observed with both HIRES and DEIMOS. The x -axis shows the high resolution spectroscopic metallicities. The y -axis shows medium resolution synthetic metallicities from this work, which are consistent with the HIRES metallicities. The dashed line is one-to-one, and the dotted lines are at ± 0.2 dex to guide the eye.

Many previous abundance studies of large samples (> 10 RGB stars) of medium-resolution spectra in MW dSphs (H06, SG07, Winnick 2003; Tolstoy et al. 2004; Koch et al. 2006, 2007a,b; Bosler et al. 2007; Battaglia et al. 2006, 2008) have relied on empirical relations between the CaT and $[\text{Fe}/\text{H}]$. These linear relations are calibrations based on globular clusters (GCs) in the metallicity range $-2.1 \lesssim [\text{Fe}/\text{H}] \lesssim -0.6$ (e.g., Rutledge et al. 1997) or individual stars in MW dSphs with a minimum $[\text{Fe}/\text{H}] = -2.5$ (Battaglia et al. 2008). All of these calibrations have been shown to be accurate in their calibrated metallicity ranges. However, all of these relations are defined such that they produce a metallicity floor at $[\text{Fe}/\text{H}] = -2.5$ to -3.5 , depending on absolute magnitude, even for a star with no Ca II absorption. Therefore, the linear CaT relations must fail at very low metallicities. In fact, 56% of the stars presented here have absolute magnitudes that yield minimum $[\text{Fe}/\text{H}]_{\text{CaT}}$ (for zero CaT EW) above -3.0 . We choose to employ a different technique to avoid the much debated issue of the metallicity at which the CaT method becomes non-linear.

Kirby, Guhathakurta, & Sneden (2008, hereafter KGS08) describe a technique to measure metallicities from moderate resolution, far-red spectra of RGB stars. The method compares an observed spectrum to a grid of synthetic spectra at a range of effective temperatures, surface gravities, and compositions. Given a photometric estimate of temperature and gravity, the $[\text{Fe}/\text{H}]$ of the synthetic spectrum with the best pixel-to-pixel match to the observed spectrum is adopted as the measured $[\text{Fe}/\text{H}]$ for the star. This approach is similar to a high-resolution spectroscopic abundance analysis.

We exclude blue horizontal branch stars and spectra for which the S/N was too low to permit a radial velocity cross-correlation measurement ($\text{S/N} \lesssim 10 \text{ \AA}^{-1}$). We transform SDSS *gri* magnitudes to Johnson-Cousins *VI*

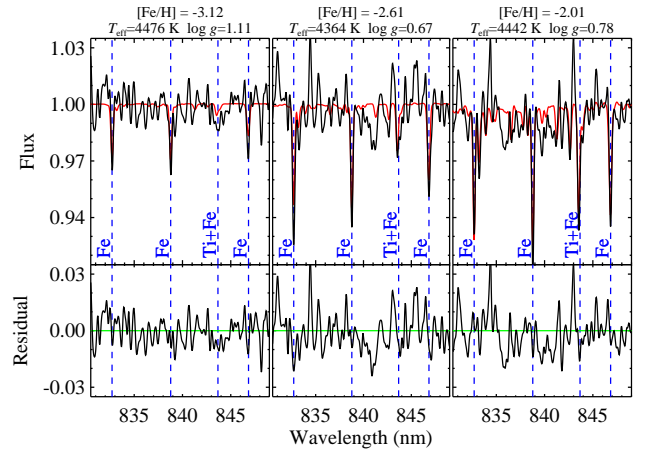


FIG. 2.— Small portions of DEIMOS spectra from three example stars at similar effective temperatures (black). The spectra are smoothed for clarity. The unsmoothed absorption line depths are about 2.3 times greater than shown here. Lines of Fe I and a Ti+Fe blend are labeled. The red lines in the top panels are synthetic spectra corresponding to the $[\text{Fe}/\text{H}]$, T_{eff} , and $\log g$ of the observed stars. In the bottom panels, the black lines are the differences between the observed and synthetic spectra, and the green lines are zero.

magnitudes following Chonis & Gaskell (2008) in order to derive the temperatures (T_{eff}) and gravities ($\log g$) in the same way as KGS08. The results are unaffected by using alternative photometric transformations. To avoid any systematic effects of varying $[\alpha/\text{Fe}]$ ratios on our $[\text{Fe}/\text{H}]$ measurements, we mask all the spectral regions susceptible to absorption by Mg, Si, S, Ar, Ca, or Ti. These regions comprise 18% of the spectral range. Future work will address $[\alpha/\text{Fe}]$ abundance ratios for these galaxies.

2.2. Assessments of the metallicities

KGS08 demonstrate their technique on Galactic GCs and show that $[\text{Fe}/\text{H}]$ may be determined as accurately as 0.1 dex on high S/N spectra and ~ 0.5 dex on spectra with S/N as low as 10 \AA^{-1} . The most metal-poor system that KGS08 analyzed is M15 ($[\text{Fe}/\text{H}] = -2.4$). To test this technique at lower metallicities, we compare our $[\text{Fe}/\text{H}]$ abundances to those determined from new Keck/HIRES spectra of several stars in UMaII and Com. The high-resolution abundance analysis of these stars (Frebel et al., in prep.) shows that the KGS08 method accurately reproduces these numbers at least down to $[\text{Fe}/\text{H}] \sim -3.0$.

Figure 1 compares synthetic metallicities to HIRES metallicities and demonstrates excellent agreement. We emphasize that the KGS08 technique is a direct measurement of a star's iron and iron-peak absorption lines and does not make use of any calibration to obtain metallicities. Therefore, it is technically not restricted to any metallicity range.

Figure 2 shows three example spectra at three different metallicities. The spectra were chosen to have similar T_{eff} and relatively high S/N. Synthetic spectra are also shown, as well as the residuals, which scatter evenly about zero except for a few upward spikes that coincide with incompletely subtracted sky emission lines. These examples demonstrate the ability for neutral iron lines to discriminate easily between stars with different (very low) metallicities even at moderate spectral resolution.

TABLE 1
ULTRA-FAINT dSPH METALLICITIES

| dSph | N^a | $\log(L/L_\odot)^b$ | $\langle[\text{Fe}/\text{H}]\rangle$ | $\sigma_{[\text{Fe}/\text{H}]}$ | $\log(\text{S}/N)^c$ |
|-------|-------|---------------------|--------------------------------------|---------------------------------|----------------------|
| UMaII | 12 | 3.6 ± 0.2 | -2.44 ± 0.06 | 0.57 | 1.5 ± 0.4 |
| LeoT | 19 | 5.1 ± 0.3 | -2.02 ± 0.05 | 0.54 | 1.1 ± 0.2 |
| UMaI | 28 | 4.1 ± 0.1 | -2.29 ± 0.04 | 0.54 | 1.5 ± 0.3 |
| LeoIV | 12 | 3.9 ± 0.2 | -2.58 ± 0.08 | 0.75 | 1.3 ± 0.3 |
| Com | 24 | 3.6 ± 0.2 | -2.53 ± 0.05 | 0.45 | 1.5 ± 0.3 |
| CVnII | 16 | 3.9 ± 0.2 | -2.19 ± 0.05 | 0.58 | 1.5 ± 0.1 |
| CVnI | 165 | 5.4 ± 0.1 | -2.08 ± 0.02 | 0.46 | 1.3 ± 0.3 |
| Herc | 22 | 4.6 ± 0.1 | -2.58 ± 0.04 | 0.51 | 1.6 ± 0.4 |

NOTE. — Data for individual stars (RA, Dec, V , I , EW_{CaT} , and $[\text{Fe}/\text{H}]_{\text{synth}}$) are available on request from the first author.

^a Number of member stars, confirmed by radial velocity, with measured $[\text{Fe}/\text{H}]$. This number is less than the total number in SG07 because we exclude spectra with $\text{S}/\text{N} \lesssim 10 \text{ \AA}^{-1}$. ^b We adopt luminosities of Martin et al. (2008) except for LeoT, for which we adopt the luminosity of de Jong et al. (2008). ^c Average spectral signal-to-noise ratio per \AA .

3. $[\text{Fe}/\text{H}]$ DISTRIBUTIONS OF THE ULTRA-FAINT DSPHS

For each dSph that SG07 observed, Table 1 shows the number of stars we analyze, mean $[\text{Fe}/\text{H}]$, the rms dispersion in $[\text{Fe}/\text{H}]$, and the distribution of S/N . The individual stellar $[\text{Fe}/\text{H}]$ values are then weighted by the inverse square of the errors and averaged to obtain the mean $[\text{Fe}/\text{H}]$ value of every dSph. These metallicity measurements establish some of our dSphs as the least enriched known stellar systems except for the MW halo, and more metal-poor than any GC.

3.1. Metal-poor tail

We have discovered for the first time stars in dSphs that are more metal-poor than $[\text{Fe}/\text{H}] = -3.0$. Our sample contains 15 such stars in seven dSphs. Only UMaII contains no stars with $[\text{Fe}/\text{H}]_{\text{DEIMOS}} < -3.0$, although it does contain two stars with $[\text{Fe}/\text{H}]_{\text{HIRES}} = -3.1$ and -3.2 . To assess the significance of these detections, we compare the metal-poor tail of the MDF for all the ultra-faint dSphs to the Fornax MDF of H06. We choose a conservative metallicity cut of $[\text{Fe}/\text{H}] < -2.0$, which includes 178 ultra-faint dSph stars and 83 Fornax stars. For each star in the metal-poor tail of the SG07 sample, we randomly select one counterpart from the metal-poor tail in Fornax. To account for the different sample sizes, some Fornax stars are used more than once. We then randomly resample the H06 $[\text{Fe}/\text{H}]_{\text{CaT}}$ measurement for each Fornax star from a normal distribution whose standard deviation is given by the uncertainty ($\delta[\text{Fe}/\text{H}]$) for its counterpart in the SG07 sample. We find that, at $[\text{Fe}/\text{H}] < -2.0$, $\delta[\text{Fe}/\text{H}]$ does not vary with metallicity.

After each star in the SG07 sample has been paired in this way, we count the number of stars with $[\text{Fe}/\text{H}] < -3.0$ in the resampled Fornax distribution. With 10^6 Monte-Carlo resampling realizations, the number distribution of stars with $[\text{Fe}/\text{H}] < -3.0$ appears roughly Poissonian with a median frequency of 5. Just 47 realizations contained at least 15 stars with $[\text{Fe}/\text{H}] < -3.0$. Therefore, we conclude that the probability that our detection of 15 stars with $[\text{Fe}/\text{H}] < -3.0$ is consistent with being drawn from the H06 Fornax MDF is very low: $P_{\text{For}} = 4.7 \times 10^{-5}$. We repeat this test with the other three H06 MDFs to determine $P_{\text{Scl}} = 3.4 \times 10^{-5}$,

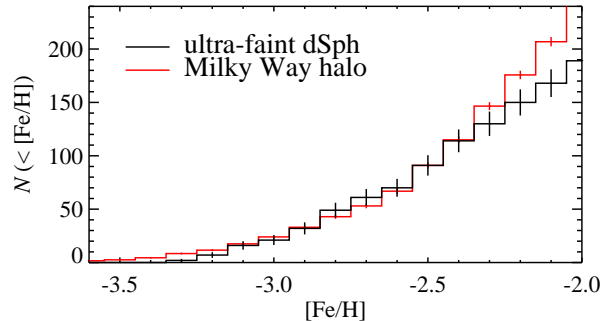


FIG. 3.— Cumulative MDFs for the metal-poor tails of the eight ultra-faint dSphs (black) and the MW halo (red, Beers et al. 2005). The red histogram is normalized to contain the same number of stars with $[\text{Fe}/\text{H}] < -2.45$ as the black histogram. The error bars are Poissonian.

$P_{\text{Car}} = 2.5 \times 10^{-5}$, and $P_{\text{Sex}} = 4.1 \times 10^{-3}$. Although Sculptor contains the lowest single-star $[\text{Fe}/\text{H}]$ measurement ($[\text{Fe}/\text{H}] = -2.86$) in the sample of H06, the Sextans MDF is most heavily weighted toward low metallicities and therefore has the highest probability of consistency with our findings of $[\text{Fe}/\text{H}] < -3.0$ stars. These statistical tests are quite conservative and do not consider that we actually detect stars as low as $[\text{Fe}/\text{H}] = -3.3$.

In light of the claim by H06 that For, Scl, Car, and Sex lack the metal-poor tail of stars that is present in the MW halo, we compare our newly measured MDF of the ultra-faint dSphs to the MW halo MDF. Figure 3 shows the metal-poor end of the halo cumulative MDF from the HK and Hamburg/ESO Surveys with carbon-enhanced stars removed (Beers et al. 2005) compared to the cumulative MDF for all eight ultra-faint dSphs combined. The halo histogram is normalized to the number of ultra-faint dSph stars with $[\text{Fe}/\text{H}] < -2.45$ in order to mute the incompleteness of the halo MDF at higher $[\text{Fe}/\text{H}]$. This rough comparison can be done more rigorously when a more complete halo MDF becomes available. In the meantime, we find that the shape of the metal-poor halo MDF agrees qualitatively with that of the ultra-faint dSph MDF. Note that the latter MDF covers a narrower dSph luminosity range than the broad range of dwarf galaxies which presumably built the stellar halo. As a result, the ultra-faint dSph MDF will cover a narrower metallicity range than the halo MDF because of the different star formation efficiencies.

Figure 4 shows the combined MDF for all eight dSphs, spanning the range $-3.3 < [\text{Fe}/\text{H}] < -0.1$. Because CVnI is significantly more luminous and more metal-rich, we also display its MDF separately.

3.2. Luminosity-metallicity relation

The segregation by luminosity of the ultra-faint dSphs, combined with our new $[\text{Fe}/\text{H}]$ measurements, leads us to re-determine the luminosity-metallicity relation for all MW dSphs except Sagittarius, which is a very metal-rich outlier. We also exclude the least luminous objects (Willman 1, Segue 1, and Boötes II) because they have only a few RGB stars, and their metallicities are not well known. Figure 5 combines $[\text{Fe}/\text{H}]$ and L for the classical dSphs with data for the ultra-faint dSphs (Table 1). Over the full 3.6 dex range of luminosity, this combined sample shows a well-defined relation. Our ultra-faint dSphs

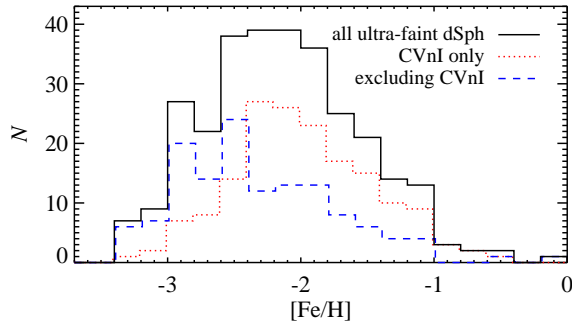


FIG. 4.— Combined MDF for all eight ultra-faint dSphs (black), for CVnI only (red dotted), and for all ultra-faint dSphs except CVnI (blue dashed). CVnI is the most luminous satellite of those presented here, and it is also the most metal-rich.

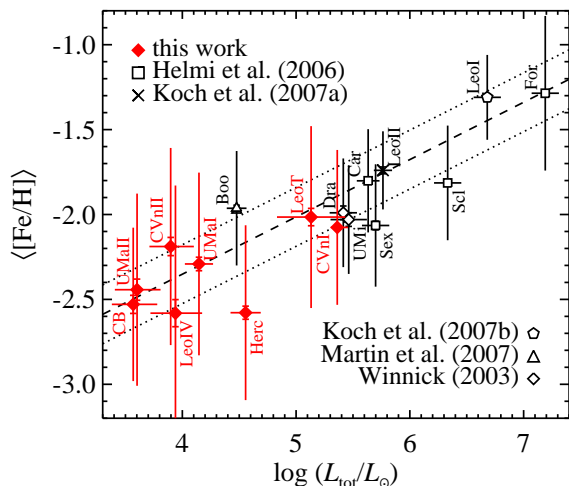


FIG. 5.— The mean $\langle [\text{Fe}/\text{H}] \rangle$ of MW dSphs vs. total luminosity. For those dSphs not listed in Table 1, we adopt the luminosities of Martin et al. (2008, Boo) and Mateo (1998, others). The figure legends give the sources of $[\text{Fe}/\text{H}]$ measurements. The dashed line is the weighted, least-squares straight line fit in $\log(L)$ - $[\text{Fe}/\text{H}]$ space, accounting for the errors in both L and $[\text{Fe}/\text{H}]$ (Akritas & Bershady 1996). The dotted lines are the rms dispersion of the residuals. The full vertical error bars are the rms dispersions of $[\text{Fe}/\text{H}]$ within a single galaxy, and the hatch marks (not visible for all dSphs) are the errors on $\langle [\text{Fe}/\text{H}] \rangle$. The MW satellite luminosity-metallicity relation is well-defined for nearly 4 dex in luminosity.

extend the trend found in the more luminous systems.

The following equation describes the fit, where the errors are the standard deviations of the slope and intercept:

$$\langle [\text{Fe}/\text{H}] \rangle = (-2.01 \pm 0.05) + (0.34 \pm 0.05) \log \left(\frac{L_{\text{tot}}}{10^5 L_{\odot}} \right)$$

The linear Pearson correlation coefficient for the data is 0.89, indicating a highly significant correlation.

4. CONCLUSIONS

We have presented metallicity measurements for eight of the least luminous known galaxies in the Universe. We also discover, for the first time, stars outside the MW field halo population with $[\text{Fe}/\text{H}] < -3.0$. Furthermore, we have shown that the distribution of $[\text{Fe}/\text{H}]$ in present-day dSphs reaches nearly as low as that of the MW stellar halo, and that the dSph luminosity-metallicity relation is well-defined for nearly 4 dex in luminosity.

There are two main differences between our study and previous works that might have contributed to our discovery of extremely metal-poor stars in MW dSphs. First, our spectral synthesis approach is valid for any metallicity and is not restricted to calibrated ranges, like the CaT technique. Second, we explored very faint dSphs whereas H06 examined more luminous dSphs. We have found extremely metal-poor stars only in the faintest dSphs. It remains to be seen whether any of the brighter dSphs also harbor extremely metal-poor stars.

$[\text{Fe}/\text{H}]$ is just one abundance puzzle in the role of dSphs in building the stellar halo. Additional elements will need to be examined to obtain further clues. Most notably, $[\alpha/\text{Fe}]$ ratios in the more luminous dSphs are on average lower than in the halo (e.g., Shetrone et al. 2003; Geisler et al. 2007). However, cosmologically motivated models including star formation and chemical enrichment (Robertson et al. 2005; Font et al. 2006) may explain the difference. These models along with the discovery of extremely metal-poor stars in long-lived dSphs support the original hierarchical paradigm of galaxy formation (e.g., Searle & Zinn 1978; White & Rees 1978).

We thank Jennifer Johnson, Kim Venn, and the referee for valuable advice. We acknowledge National Science Foundation grants AST-0307966 and AST-0607852 and NASA/STScI grants GO-10265.02 and GO-10134.02. E. N. K. is supported by a NSF Graduate Research Fellowship. A. F. acknowledges support through the W. J. McDonald Fellowship of the McDonald Observatory.

Facility: Keck:II (DEIMOS)

REFERENCES

- Akritis, M. G., & Bershady, M. A. 1996, *ApJ*, 470, 706
 Battaglia, G., Irwin, M., Tolstoy, E., Hill, V., Helmi, A., Letarte, B., & Jablonka, P. 2008, *MNRAS*, 383, 183
 Battaglia, G., et al. 2006, *A&A*, 459, 423
 Beers, T. C., et al. 2005, *From Lithium to Uranium: Elemental Tracers of Early Cosmic Evolution*, 228, 175
 Bosler, T. L., Smecker-Hane, T. A., & Stetson, P. B. 2007, *MNRAS*, 378, 318
 Bullock, J. S., & Johnston, K. V. 2005, *ApJ*, 635, 931
 Choi, P. I., Guhathakurta, P., & Johnston, K. V. 2002, *AJ*, 124, 310
 Chonis, T. S., & Gaskell, C. M. 2008, *AJ*, 135, 264
 de Jong, J. T. A., et al. 2008, *ApJ*, 680, 1112
 Font, A. S., Johnston, K. V., Bullock, J. S., & Robertson, B. E. 2006, *ApJ*, 638, 585
 Geisler, D., Wallerstein, G., Smith, V. V., & Casetti-Dinescu, D. I. 2007, *PASP*, 119, 939
 Gilbert, K. M., et al. 2007, *ApJ*, 668, 245
 Guhathakurta, P., et al. 2006, *AJ*, 131, 2497
 Helmi, A., et al. 2006, *ApJ*, 651, L121
 Howley, K. M., Geha, M., Guhathakurta, P., Montgomery, R. M., Laughlin, G., & Johnston, K. V. 2008, *ApJ*, in press (arXiv:0804.0798)
 Ibata, R. A., Gilmore, G., & Irwin, M. J. 1994, *Nature*, 370, 194
 Ibata, R. A., Ferguson, J., & Tanvir, A. 2001, *Nature*, 412, 49
 Kirby, E. N., Guhathakurta, P., & Sneden, C. 2008, *ApJ*, 682, 1217

- Koch, A., Grebel, E. K., Kleyna, J. T., Wilkinson, M. I., Harbeck, D. R., Gilmore, G. F., Wyse, R. F. G., & Evans, N. W. 2007a, *AJ*, 133, 270
- Koch, A., Grebel, E. K., Wyse, R. F. G., Kleyna, J. T., Wilkinson, M. I., Harbeck, D. R., Gilmore, G. F., & Evans, N. W. 2006, *AJ*, 131, 895
- Koch, A., Wilkinson, M. I., Kleyna, J. T., Gilmore, G. F., Grebel, E. K., Mackey, A. D., Evans, N. W., & Wyse, R. F. G. 2007b, *ApJ*, 657, 241
- Martin, N. F., de Jong, J. T. A., & Rix, H.-W. 2008, *ArXiv e-prints*, 805, arXiv:0805.2945
- Martin, N. F., Ibata, R. A., Chapman, S. C., Irwin, M., & Lewis, G. F. 2007, *MNRAS*, 380, 281
- Mateo, M. L. 1998, *ARA&A*, 36, 435
- Robertson, B., Bullock, J. S., Font, A. S., Johnston, K. V., & Hernquist, L. 2005, *ApJ*, 632, 872
- Rutledge, G. A., Hesser, J. E., & Stetson, P. B. 1997, *PASP*, 109, 907
- Searle, L., & Zinn, R. 1978, *ApJ*, 225, 357
- Shetrone, M. D., Côté, P., & Sargent, W. L. W. 2001, *ApJ*, 548, 592
- Shetrone, M., Venn, K. A., Tolstoy, E., Primas, F., Hill, V., & Kaufer, A. 2003, *AJ*, 125, 684
- Simon, J. D., & Geha, M. 2007, *ApJ*, 670, 313
- Tolstoy, E., Irwin, M. J., Cole, A. A., Pasquini, L., Gilmozzi, R., & Gallagher, J. S. 2001, *MNRAS*, 327, 918
- Tolstoy, E., et al. 2003, *AJ*, 125, 707
- Tolstoy, E., et al. 2004, *ApJ*, 617, L119
- White, S. D. M., & Rees, M. J. 1978, *MNRAS*, 183, 341
- Winnick, R. A. 2003, Ph.D. Thesis, Yale Univ.